ISSN: 2754-4753

Journal of Physics & Optics Sciences

SCIENTIFIC Research and Community

Research Article

Open Access

Study on the Physical Properties of Pulsed Laser Deposited Doped Copper Oxide (Cu_2O) Thin Films for Optical Device Applications

Gurpreet Kaur and Anirban Mitra

High Power Laser Lab, Department of Physics, Indian Institute of Technology Roorkee, Roorkee-247667, Uttarakhand, India

ABSTRACT

Cuprous oxide, (Cu_2O) is a promising p-type semiconductor, finds practical applications in a wide range of optoelectronic devices. In this paper, pulsed laser deposition technique is employed to deposit doped Cu_2O thin films. The influence of doping of silver (Ag), aluminium (Al) and co-doping of (Ag+Al) in Cu_2O thin films is illustrated. X-ray diffraction pattern depicts cubic crystal structure and polycrystalline nature of grown thin films, having small crystallite size (~50 nm). Atomic force microscopy (AFM) obtained surface images of the films portrait uniform grain morphology with low surface roughness. The room temperature optical characterizations of the thin films, the transmittance versus wavelength in the UV-Visible region exhibits low transmission values upto 10–20%, illustrates the large absorption coefficient (α), numerical values varying from 10^4 to 10^5 cm^{-1} for doped Cu_2O films. The large values of absorption coefficient facilitate the optical and photovoltaic applications of the doped Cu_2O films. The addition of dopant species Ag and Al, the optical band gap is increased and it varies in the range of 2.65–2.84 eV. The increased energy gap is attributed to the substitution of Al and Ag ions for the oxygen ions reduce the width of valence band to widen the energy gap. The I–V characteristics plot obtained at room temperature indicates low electrical resistivity ($\rho \sim 10^{-2}$ Ω- cm) of the films. The obtained results are of high relevance and indicate potential applications of the grown thin films in semiconductor devices such as solar cells, photodetectors and optical sources.

***Corresponding author**

Gurpreet Kaur, High Power Laser Lab, Department of Physics, Indian Institute of Technology Roorkee, Roorkee-247667, Uttarakhand, India, Email: physgk@gmail.com, gkaurdnt@iitrernet.in

Received: December 18, 2020; **Accepted:** December 28, 2020; **Published:** December 31, 2020

Keywords: Thin Films, Pulsed Laser Deposition, Resistivity, Optical Transmittance, Band Gap

Introduction

Metal oxide semiconductors are used in wide range of devices such as: solar cells, thin film transistors, photodetectors and light-emitting diodes [1-7]. Cu_2O is a natural p-type semiconductor having direct band gap of 2.1-2.5 eV with brownish-red color and a semi- transparent light absorber [5, 8]. Cu_2O has drawn attention for optoelectronic devices due to its large absorption coefficient, unique electronic structure, fair electrical conductivity at room temperature, wide availability and non-toxic nature [9-12]. The Shockley-Queisser, theoretical energy conversion efficiency is about 20% for Cu_2O based solar cells [5, 7].

Cu_2O shows spontaneous p-type conductivity due to the presence of cation (Cu^+) vacancies and the oxygen interstitials, (Oi) in its structure. Due to these defects the acceptor level or hole states are created above the valence band [13]. The acceptors with energies 0.25 to 0.4 eV are arising from Cu vacancies. The concentration of stable copper vacancies (V_{Cu}) is ~10^{20} cm^{-3}, but not all VCu are ionized to generate free holes. At room temperature concentration of free holes is ~$10^{18}cm^{-3}$ [14]. The manifesting physical properties of Cu_2O result from its excitonic structure, owing to relatively large binding energy of free excitons i.e. 150 meV [13]. The excitons are characterized by larger lifetimes >10 μsec in Cu_2O [13]. Cu_2O has a longer minority carrier diffusion length (~5 μm), than most of the metallic oxides [13, 7]. Cu_2O suffers with a low transparency, which can be improved by cation doping [15]. In the band structure of Cu_2O, valence band is formed by fully filled d-orbitals of copper cations, along with 2p-orbitals of oxygen anions, the bonding between Cu and O atoms allow sizeable covalency and results in the formation of a delocalized valence band edge [16].

Cu_2O possess simple cubic, cuprite crystal structure with space group Pn3m No. 224 [14] and lattice constant a=4.27 Å [11, 17]. It can be formed by interpenetration of two sublattices, a face centered cubic (fcc) sublattice of copper cations and a body-centered cubic (bcc) sublattice of oxygen anions. In Cu_2O lattice, each Cu atom is coordinated with two O atoms and D3d site symmetry [9, 14]. Each O atom has four Cu atom neighbors with Td site symmetry in a tetrahedral arrangement [16-17]. Oxygen atoms occupy tetrahedral interstitial positions relative to the copper sublattice [16].

The properties of Cu_2O can be enhanced by doping of external atoms [18]. It is practically not easy to achieve n-type doping due to self-compensation mechanism in Cu_2O [3]. Several elements are found to be efficient p-type dopants for Cu_2O, such as, silicon (Si), nitrogen (N) and silver (Ag) [8, 18-20].

In this paper, we report the growth and physical properties of doped Cu_2O thin films deposited by Pulsed laser deposition (PLD)

technique. The effects of Aluminium (Al), silver (Ag) doping and (Al+Ag) co-doping in Cu_2O thin films, consecutively their optical and electrical properties are investigated precisely.

Experimental Details

Growth of Thin Films

Doped Cu_2O thin films are grown by Pulsed laser deposition technique (PLD). An Nd:YAG laser operating at wavelength 355 nm and energy 100 mJ/pulse is used to ablate the targets. The highly energetic, short duration (9 nsec) laser pulses are focused on the target which leads to the rapid evaporation of the target materials. The evaporated materials consist of highly excited and ionized species, known as plasma plume. The condensation of the ablated plasma species results in thin film formation on the substrate. The Al, Ag doped and (Al+Ag) co-doped Cu_2O targets are prepared by the solid state reaction method. By mixing Cu_2O powder with Al_2O_3 and Ag_2O, powders respectively taken in stoichiometric ratios. The doping profile for both Al and Ag in Cu_2O is kept 5%. For co-doped it is 2.5% Al and 2.5% Ag in Cu_2O. The powders are thoroughly mixed and grinded for 2 hours using a mortar and pestle. These homogeneous powders are pressed into a disk, called pallet of diameter 20 mm and thickness about 5 mm, by applying 20 ton force with a hydraulic press. The PLD targets of Cu_2O:Al, Cu_2O:Ag and Cu_2O:Al:Ag are prepared by sintering the powder pallets at 600 °C in argon atmosphere for 1 hour. The deposition parameters are optimized to obtain good quality of thin films. The stainless steel vacuum chamber is initially evacuated upto 10-5 Pa. The substrate temperature for depositing thin films is kept constant at 400 °C, oxygen gas pressure 1.33 Pa (10 mTorr) and time of deposition is kept 30 minutes. The deposition rate of 10 nm/minute is kept to obtain 300 nm thick films. All the films were deposited using third harmonic of Nd:YAG laser operating at 355 nm with pulse repetition rate 10 Hz and pulse duration of 10 nsec. Energy per pulse of the laser was kept at 150 mJ and the focused spot size onto the target was ~500 μm2.

Characterizations of the Deposited Thin Films

The crystal structure of the deposited films is analyzed by X-ray diffractometer (Bruker AXS D8 Advanced) in θ–2θ mode with CuKα radiation (λ = 0.154 nm). The surface morphology and roughness analysis of the as grown films is examined by Atomic Force Microscopy (NT- MDT: Model Ntegra), in semi-contact mode using Silicon Nitride tip of radius 10 nm. Room temperature UV-Visible optical transmission versus wavelength behavior of the grown films is analyzed by UV-1800 SHIMADZU, UV-VIS Spectrophotometer. The spectrophotometer is used in double beam mode with air as a reference medium. Thus, transmission spectrum is obtained by subtracting the absorption value of the glass substrate. The optical band gap of the films is calculated from Tauc's plot relation. The electrical properties, current-voltage (I-V) behavior of the deposited films is observed by Keithley 4200 SCS using four point probe resistivity method.

Results and Discussion

X-ray Diffraction Studies for Crystal Structure Analysis

The room temperature X-ray diffraction, (XRD) pattern of the grown thin film samples is indicated by Figure 1. XRD data plots illustrate the poly-crystalline nature of the films, with a cubic crystal structure. The XRD peaks are indexed by comparing the data with JCPDS card file No. 75-1531. XRD data for thin films reveal pure Cu_2O phase formation, no other impurity like CuO or Cu peaks are detected. The intensity of XRD peak is a direct measure of crystallinity. The crystallite size (l) of the grown films is estimated by using the Debye-Scherrer empirical formula [13]:

$$l = \left(\frac{0.9\lambda}{\beta cos\theta}\right) \quad \text{.....(1)}$$

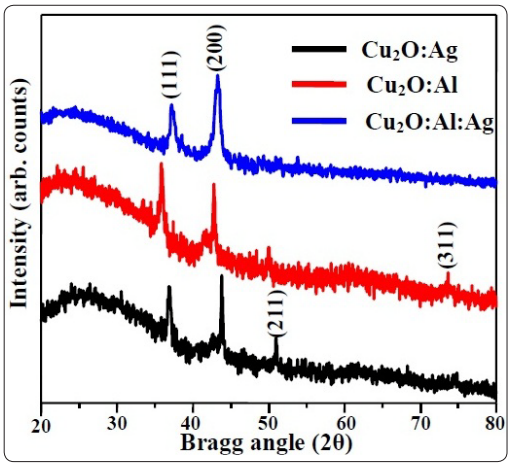

Figure 1: XRD patterns of the deposited thin films indicating crystalline nature

Where λ=0.154 nm, is the wavelength of X-rays used, β is the full width at the half maxima of the XRD peak (200) and θ is the Bragg diffraction angle. The crystallite size represents dimension of the coherent diffracting domain. The calculated values of crystallite size (*l*) are given in Table 1. The values of l are found to be <70 nm, indicate good crystalline nature of thin films, also it favors the electrical conductivity properties of films. The structural properties and particle distribution on the film surface strongly influence the optical and hence the electrical properties.

Table 1: Structural parameters calculated from XRD data analysis: lattice spacing, lattice constant, Texture coefficient for peak (111) and (200), Crystallite size along (200)

Sample	Lattice spacing d(111) nm	Lattice constant a(111) nm	Texture coefficient (111)	Texture coefficient (200)	Crystallite size, l nm
Cu_2O:Ag	0.243	0.421	0.897	1.869	62.25
Cu_2O:Al	0.251	0.435	1.098	1.432	59.41
Cu_2O:Al:Ag	0.242	0.419	0.938	1.941	38.74

The lattice parameters, inter-planar spacing (d) is given by Bragg's law condition and the obtained lattice constant is related by the following equation [7]:

$$d = \frac{a}{\sqrt{h^2 + k^2 + l^2}} \quad \text{.....(2)}$$

Here h, k and l represents the value of Miller indices for the particular plane. The values of calculated lattice parameters and crystallite size are given in Table 1.

The structure and preferred orientation of the deposited doped Cu_2O thin films are examined in detail, the texture coefficient (TC) of preferred orientation is determined by the Harris formula, which is defined as [7, 12]:

$$TC(hkl) = \frac{[I(hkl)/I_0(hkl)]}{\left[N^{-1}\sum_n I(hkl)/I_0(hkl)\right]} \quad \text{.....(3)}$$

Here, N is the number of diffraction peaks in the pattern, I(hkl) describe the measured relative intensity of a plane and I_0(hkl) denote the standard intensity of the plane (hkl) taken from JCPDS data files, containing textured and randomly oriented grains, respectively. The value TC = 1 represents films with randomly oriented crystallites, whereas higher values indicate an abundance of grains oriented in a given (hkl) direction [7]. The values of TC(111) and TC(200) are calculated using equation 3, and are given in Table 1.

Surface Morphology and Roughness estimation from Atomic Force Microscopy data analysis:

The AFM obtained surface topography is indicated by Figure 2. The doped Cu_2O thin films comprise uniformly distributed, with nano-scale dimensions of the grains. The three dimensional (3-D) AFM images, describe the dense and homogeneous surface morphology of doped Cu_2O thin films with low surface roughness. The z-dimension shows the particle heights of formed nano-grains. These grains have well-defined shape (nano pillars) oriented along (200) plane, uniform particle size and good dispersion on the film surface. For a quantitative evaluation of the surface topography, the average and root mean square (RMS) roughness are calculated from the AFM analysis is given mathematically by the following relationships [7]:

$$R_{avg} = \frac{1}{N}\sum_{i=1}^{N}\left|Z_i - \bar{Z}\right| \quad \text{.....(4)}$$

$$R_{rms} = \frac{1}{N}\left[\sum_{i=1}^{N}\left|Z_i - \bar{Z}\right|^2\right]^{1/2} \quad \text{.....(5)}$$

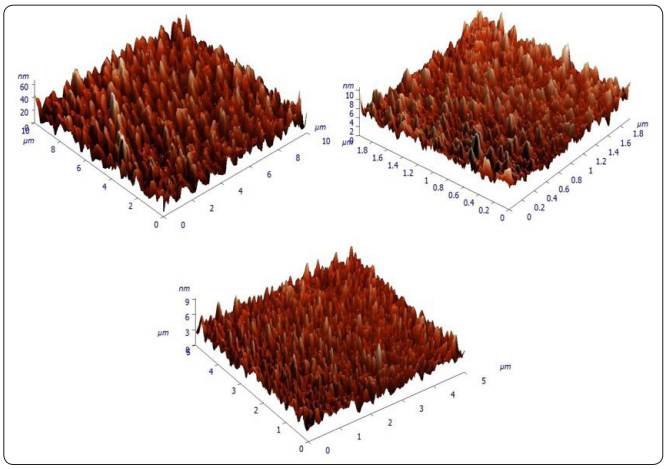

Figure 2: Three dimensional (3-D) view of the film surface obtained from Atomic force microscopy

Here, N is the number of surface height data and z is the mean-height distance. The surface coverage is given by the ratio of area covered by all the grains to the total scanned area (in μm^2). The calculated micro-structural parameters i.e. aspect ratio of the particles, particle density given by number of particles per unit area, surface coverage estimated from the ratio of area covered by the grains to the total scanned area and roughness values obtained from AFM data analysis are given in Table 2. The surface roughness and dislocation boundary play a crucial role in the optical and electrical properties, by affecting optical absorption and mobility of charge carriers in thin films.

Table 2: Surface morphology and grain parameters evaluated from AFM data analysis: Aspect ratio, Particle density, Surface coverage and Surface roughness of the as grown thin films

Sample	Mean height h (nm)	Mean diameter D (nm)	Aspect ratio D/h	Particle Density ($1/cm^2$)	Surface coverage (%)	Roughness (nm)	
						Average	Rms
Cu_2O:Ag	26.64	53.76	2.02	12.2×109	71.47	20.9	20.47
Cu_2O:Al	10.37	24.57	2.37	18.3×109	83.25	7.23	6.98
Cu_2O:Al:Ag	8.07	18.82	2.33	17.6×109	81.65	5.12	4.17

UV-Visible Optical Spectroscopy

The optical transmittance spectra of the doped Cu_2O films in the UV-visible region are illustrated in Figure 3. The thin films exhibit transparency in NIR region, and a strong absorption edge below 500 nm, due to the band gap of Cu_2O. The thin films exhibit low transmittance below band gap i.e. 10–20%, due to the large absorption coefficient (α) of Cu_2O. The large values of α demonstrate the photovoltaic and optical applications of these doped Cu_2O films. The maxima and minima in the transmittance curve are caused by the interference between the two beams of light reflected from the air-film and film-glass interfaces. These fringes formed in the transmittance spectrum are helpful in calculating the thickness of the thin films, according to the following equation [21]:

$$t = \frac{\lambda_1\lambda_2}{2\left[\lambda_1 n_1 - \lambda_2 n_2\right]} \quad \text{.....(6)}$$

Here λ_1, λ_2 are the wavelengths of adjacent minima or maxima (nm) in the transmittance spectrum, and n_1, n_2 are the refractive indices of the film at λ_1 and λ_2 respectively. For the Cu_2O thin films, the refractive indices were assumed to be approximately equal ($n_1 \approx n_2$), as this difference is very small in the visible region. The film thickness is estimated at the absorption edge, i.e. 500 nm taking value of $n_1 = n_2 = 3.446$ [23], calculated values of film thickness are given in Table 3. The doped Cu_2O films exhibit lower transmittance (% values) as compared with pure Cu_2O films, due to free carrier absorption from the dopant species which lowers the

transmittance. The transmittance is quite low for Ag-doped Cu_2O films, explicit the increase in absorption of light with the addition of Ag, this may be attributed to the creation of electron–hole pairs or atomic vibration, interface effect or plasmonic effects [8].

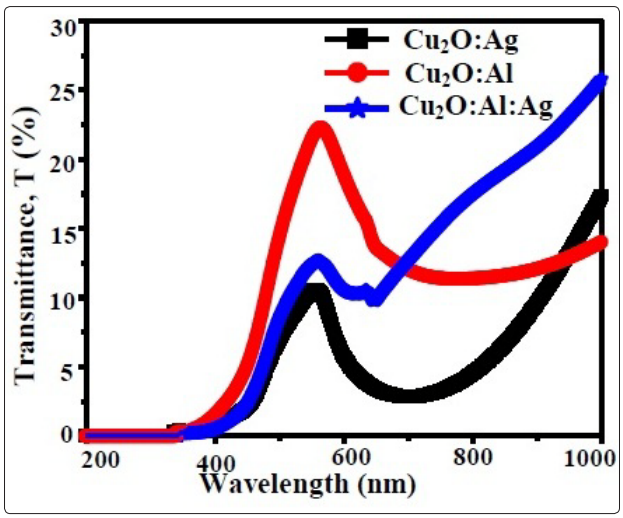

Figure 3: Optical transmittance versus wavelength spectra for the doped Cu_2O thin films

Table 3: Calculated values of film thickness (t), Energy band gap (Eg) from optical data and Electrical resistivity from I-V characteristics

Sample	Thickness t (nm)	Band gap Eg (eV)	Resistivity Resistivity
Cu_2O:Ag	305.9	2.73	6.53×10^{-2}
Cu_2O:Al	313.4	2.84	12.24×10^{-2}
Cu_2O:Al:Ag	354.1	2.65	4.54×10^{-2}

The absorption coefficient α is obtained from UV-Visible optical transmittance data using the equation [8]:

$$\alpha = \frac{1}{t}\ln\left(\frac{1}{T}\right) \quad \text{.....(7)}$$

The parameter T is the optical transmittance values at a particular frequency. The value for absorption coefficient is quite large in the visible region, α lies in the range of 10^4 cm^{-1} to 10^5 cm^{-1} which is good for solar cell applications. The Figure 4 represents the variation of absorption coefficient (α) versus energy (hν), corresponding to a particular wavelength.

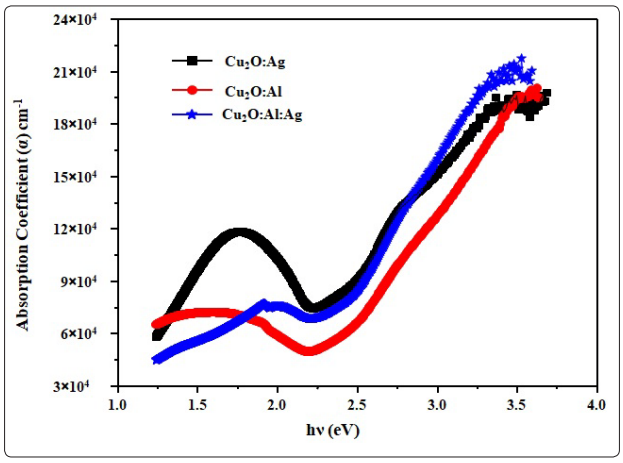

Figure 4: The variation of Absorption coefficient (α) versus energy (hν), for doped Cu_2O thin films

The energy band gap of the doped Cu_2O films is approximated from Tauc's plot expression, given by the following mathematical equation [7, 8]:

$$\alpha = \frac{A\left(E - E_g\right)^n}{E} \quad \text{.....(8)}$$

Where A is the constant, E = hν is the photon energy, E_g is the band gap. The value of n is taken as 1/2 for direct allowed transitions. Tauc's plot is plotted as $(\alpha h\nu)^2$ versus hν. The band gap, E_g is obtained by extrapolating the linear portion of the curve to the energy axis at $(\alpha h\nu)^2 = 0$, shown in Figure 5. The calculated values of band gap (Eg) are recorded in Table 3.

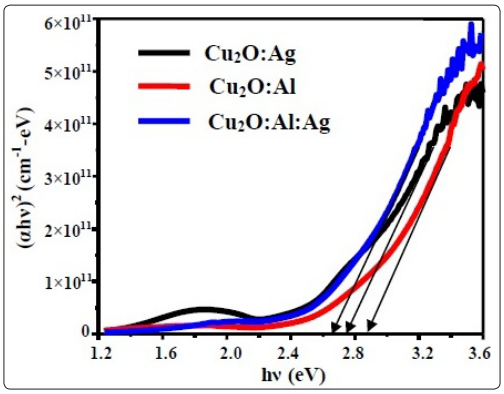

Figure 5: Optical Energy band gap calculated from Tauc's plot relation, representing direct band gap for the grown thin films

It is found that the doped Cu_2O films exhibit large band gap than the pure Cu_2O (~2.3 eV) films [12, 22]. The increased band gap of doped Cu_2O thin films is attributed to the substitution of Al and Ag ions for the oxygen ions. Due to this substitution width of the valence band is reduced to enlarge the band gap. Similar results are reported previously for N-doping [19]. It is also observed that the doping induced structural distortions, distrupt the Cu–Cu interactions around the dopant and increase the band gap for the doped Cu_2O [15, 16]. The optical properties of the crystalline semiconductors are strongly influenced by the atomic arrangement, structural parameters and the defect states, as crystalline defects are increased significantly by the doping phenomena therefore it alters the band gap.

Current-Voltage Characteristics

The four point probe method is used to obtain resistivity of the doped Cu_2O thin films. The current-voltage (I−V plot) characteristics for the as deposited thin films is shown in Figure 6, it indicates ohmic conduction behavior in the voltage sweep of -1 V to +1 V. In Cu_2O, natural p-type behavior comes from the Cu-vacancies (V_{Cu}) or oxygen interstitials (O_i) in the lattice structure [11]. Owing to these structural defects hole states are introduced, in the form of acceptor levels or trap levels lying above the top of the valence band [4, 13]. The electrical properties are primarily controlled by the defect states. The thin film resistivity (ρ) is estimated from four probe resistivity method, using this relation [7, 19]:

$$\rho = \frac{\pi t}{\ln 2} \times \left(\frac{V}{I}\right) \quad \text{.....(9)}$$

Where t is the film thickness kept 300 nm and the factor (π/ln2)×R is called the sheet resistance (R_{sh}). The evaluated values of ρ are given in Table 3. The doped Cu_2O films show enhanced electrical conductivity, which enables their practical applicability for p-channel oxide thin-film transistors (TFTs) [4]. For practical

applications of doped Cu_2O films, it is necessary to control electrical properties, the free holes carrier density [18].

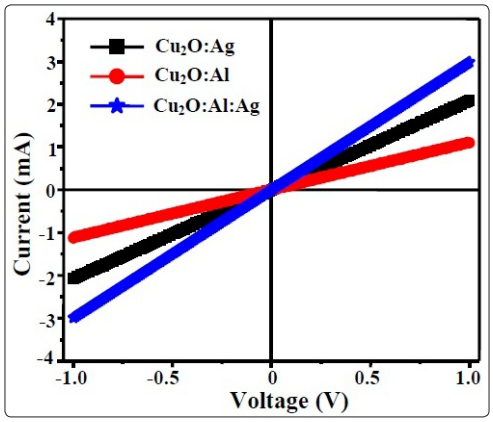

Figure 6: The room temperature current-voltage (I−V), behavior from Four Probe measurements indicates ohmic conduction in the thin films

The good crystallinity of the films decreases the defect centers such as micro-cracks and dislocation density or grain boundaries which interrupt the charge carriers flow and affects the mobility of charge carriers [4]. The carrier mobility may be affected by the crystal orientation owing to effective mass anisotropy [7]. Thus, the thin film conductivity is directly influenced by its crystalline nature grown microstructures inside the film and its morphology [3, 7]. The optical and electrical properties of semiconductor thin films are also modified by the nano-sized crystallites due to quantum size effects [7].

Conclusions

In this report Al, Ag doped and (Al+Ag) co-doped Cu_2O thin films are successfully grown on glass substrates using PLD techniques. The crystallographic, optical and electrical properties of the as deposited doped Cu_2O films are investigated systematically. The thin films possess cubic crystal structures with (111) and (200) plane orientations. The sharp and intense peaks of XRD pattern reveal the good crystalline nature of films. The optical spectroscopy indicates low transmission and a large absorption coefficient values for the grown films. Doping in Cu_2O increases the band gap of the deposited thin films. The I−V characteristics curve indicates the ohmic behavior in the films, with a low resistivity. Electrical properties of Cu_2O are improved by doping of external atoms, Al and Ag. All these findings would be useful for the optimization and growth of Cu_2O thin films for their significant optical and photovoltaic or optoelectronic device applications. The doped Cu_2O thin films with improved physical properties can be used for low-cost electronic devices such as thin film transistors.

Acknowledgments

The authors would like to acknowledge the Department of Science and Technology (DST), Government of India, for their financial support of INSPIRE fellowship in doing this research work.

References

1. Norton DP (2004) Synthesis and properties of epitaxial electronic oxide thin-film materials. Materials Science and Engineering R: Report 43:139-247.
2. Kaur G, Yadav KL, Mitra A (2015) Localized surface plasmon induced enhancement of electron-hole generation with silver metal island at n-Al:ZnO/p-Cu2O heterojunction. Applied Physics Letters 107: 53901.
3. Chen J-W, Perng D-C, Fang J-F (2011) Nano-structured Cu2O solar cells fabricated on sparse ZnO nanorods. Solar Energy Materials and Solar Cells 95: 2471-2477.
4. Yao ZQ, Liu SL, Zhang L, He B, Kumar A, et al. (2012) Room temperature fabrication of p-channel Cu2O thin-film transistors on flexible polyethylene terephthalate substrates. Applied Physics Letters 101: 042114.
5. Hsueh T-J, Hsu C-L, Chang S-J, Guo P-W, Hsieh J-H, et al (2007) Cu2O/n- ZnO nanowire solar cells on ZnO:Ga/glass templates. Scripta Materialia 57: 53-56.
6. Ok YH, Lee KR, Jung BO, Kwon YH, Cho HK (2014) All oxide ultraviolet photodetectors based on a p-Cu2O film/n-ZnO heterostructure nanowires. Thin Solid Films, 570, pp. 282-287.
7. Kaur G, Mitra A, Yadav KL (2015) Influence of oxygen pressure on the growth and physical properties of pulsed laser deposited Cu2O thin films. Journal of Materials Science: Materials in Electronic, 26: 9689-9699.
8. Tseng CC, Hsieh JH, Wu W (2011) Microstructural analysis and optoelectrical properties of Cu2O, Cu2O–Ag, and Cu2O/Ag2O multilayered nanocomposite thin films. Thin Solid Films, 519: 5169-5173.
9. Amekura H, Umeda N, Takeda Y, Kishimoto N (2006) Optical transitions of Cu2O nanocrystals in SiO2 fabricated by ion implantation and two-step annealing. Applied Physics Letters, 89: 223120.
10. Lyubinetsky I, Thevuthasan S, McCready DE, Baer DR (2003) Formation of single-phase oxide nanoclusters: Cu2O on SrTiO3(100). Journal of Applied Physics, 94: 7926-7928.
11. Valladares LD, Salinas DH, Dominguez AB, Najarro DA, Khondaker SI, et al. (2012) Crystallization and electrical resistivity of Cu2O and CuO obtained by thermal oxidation of Cu thin films on SiO2/Si substrates. Thin Solid Films 520: 6368-6374.
12. Nagai H, Suzuki T, Hara H, Mochizuki C, Takano I, et al. (2012) Chemical fabrication of p-type Cu2O transparent thin film using molecular precursor method. Materials Chemistry and Physics 137: 252-257.
13. Karapetyan A, Reymers A, Giorgio S, Fauquet C, Sajti L, et al. (2015) Cuprous oxide thin films prepared by thermal oxidation of copper layer. Morphological and optical properties. Journal of Luminescence 159: 325-332.
14. Raebiger H, Lany S, Zunger A (2007) Origins of the p-type nature and cation deficiency in Cu2O and related materials. Physical Review B 76: 045209.
15. Nolan M, Elliott SD (2008) Tuning the Transparency of Cu2O with Substitutional Cation Doping. Chemistry of Materials 20: 5522-5531.
16. Hu JP, Payne DJ, Egdell RG, Glans P.-A, Learmonth T, et al. (2008) On-site interband excitations in resonant inelastic x-ray scattering from Cu2O. Physical Review B 77: 155115.
17. Landolt H, Bornstein R (1998) Non-Tetrahedrally Bonded Elements and Binary Compounds I. Springer Berlin Heidelberg Press.
18. Ishizuka S, Kato S, Okamoto Y, Akimoto K (2002) Control of hole carrier density of polycrystalline Cu2O thin films by Si doping. Applied Physics Letter, 80: 950.
19. Kaur G, Dewasi A, Mitra A, Yadav KL (2016) Effect of Nitrogen Gas Annealing on the Properties of Pulsed Laser Deposited Cu2O Thin Films. Advanced Science Letters 22: 905-910.
20. Tseng CC, Hsieh JH, Liu SJ, Wu W (2009) Effects of Ag contents and deposition temperatures on the electrical and optical behaviors of Ag-doped Cu2O thin films. Thin Solid

Films 518: 1407-1410.

21. Kaur G, Mitra A, Yadav KL (2015) Influence of beam energy on the properties of pulsed laser deposited Al-doped ZnO thin films. IEEE Transactions. Nanotechnology 14: 922-930.
22. Malerba C, Biccari F, Ricardo CL A, D'Incau M, Scardi P, et al. (2011) Absorption coefficient of bulk and thin film Cu2O. Solar Energy Materials and Solar Cells 95: 2848-2854.
23. Zhang L, McMillon L, McNatt J (2013) Gas-dependent bandgap and electrical conductivity of Cu2O thin films. Solar Energy Materials and Solar Cells 108: 230-234.